Inorganic Chemistry

Article

pubs.acs.org/IC

Multifunctional Radical-Doped Polyoxometalate-Based Host–Guest Material: Photochromism and Photocatalytic Activity

Jian-Zhen Liao,[†,‡] Hai-Long Zhang,[†,‡] Sa-Sa Wang,[†] Jian-Ping Yong,[†] Xiao-Yuan Wu,[†] Rongmin Yu,[†] and Can-Zhong Lu*[,†]

[†]Key Laboratory of Design and Assembly of Functional Nanostructures, Fujian Institute of Research on the Structure of Matter, Chinese Academy of Sciences, Fuzhou, Fujian 350002, P. R. China

[‡]Graduate University of Chinese Academy of Sciences, Beijing 100049, P. R. China

Supporting Information

ABSTRACT: An effective strategy to synthesize multifunctional materials is the incorporation of functional organic moieties and metal oxide clusters via self-assembly. A rare multifunctional radical-doped zinc-based host–guest crystalline material was synthesized with a fast-responsive reversible ultraviolet visible light photochromism, photocontrolled tunable luminescence, and highly selective photocatalytic oxidation of benzylic alcohols as a result of blending of distinctively different functional components, naphthalenediimide tectons, and polyoxometalates (POMs). It is highly unique to link π-electron-deficient organic tectons and POMs by unusual POMs anion–π interactions, which are not only conducive to keeping the independence of each component but also effectively promoting the charge transfer or exchange among the components to realize the fast-responsive photochromism, photocontrolled tunable luminescence, and photocatalytic activity.

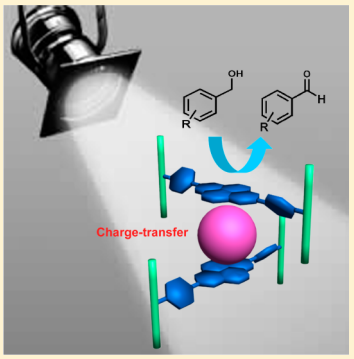

INTRODUCTION

Multifunctional crystalline organic–inorganic hybrid materials, especially the photochromic and photocatalytic materials, have attracted considerable interest because of their potential applications in photomechanics, information storage, optical switches, green catalysis technologies, etc.[1] By incorporation of functional organic moieties and metal oxide clusters via self-assembly, grafting, or intercalation, such hybrid structures are formed with multiple functionalities and often new features as a result of blending of distinctively different components.[2] It is of interest to select the appropriate functional building modules to effectively construct multifunctional crystalline solid materials with a suitable structural before researching their properties.

The electrochemical, photophysical, photochemical, and catalytic multifunctional naphthalenediimide (NDI) dye derivatives are known to be a class of excellent candidates of π-electron-deficient organic tectons for construction of multifunctional crystalline materials or metal–organic frameworks (MOFs) due to the controllability of the substituent group on the diimide nitrogens and the reversibility of the electron transfer of the naphthalene ring.[3] Polyoxometalates (POMs) are prominent building blocks to design multifunctional materials owing to their numerous advantageous properties; for instance, POMs are good electron reservoirs that exhibit rich redox and photoactivity, which undergo potential photo- or electron-induced electron- and proton-transfer processes, which can be used to build photochromic or electrochromic materials.[4] Particularly, some POMs themselves are catalytically effective and have been used as all-important components toward design and synthesis of various effective catalytic materials.[5] However, only a small number of POM-based host–guest crystalline coordination polymers used as heterogeneous catalysts have been reported;[2a,6] multifunctional crystalline materials with both photochromic and photocatalytic properties have rarely been reported to date,[7] let alone radical-doped POM-based host–guest multifunctional crystalline solid material.

Taking advantage of electronic complementary effects and popular anion–π interactions, we previously reported for the first time that multifunctional electron reservoirs (i.e., POMs) could be captured by π-electron-deficient NDIs-based coordination complexes through neoteric POMs anion–π interactions.[8] Herein, an extremely rare radical-doped zinc-based material based on functional linear NDI tectons and POM molecules was synthesized with a fast-responsive reversible photochromism, which obviously derived from the coactions of naphthalene diimide and POMs, as well as excellent photocatalytic activity toward the selective oxidation of benzylic alcohol under ambient conditions irradiated by simulated sunlight. It should be pointed out that the POMs molecules were embedded into the coordination polymers through ingenious anion–π interaction and hydrogen bonds, which not only effectively immobilize and disperse the POMs but promote the charge transfer or exchange among NDI center, coordinated other molecules and POMs surface to realize the reversible photochromism, photocontrolled tunable luminescence, and maintain efficient photocatalytic performance. To

Received: January 7, 2015

DOI: 10.1021/acs.inorgchem.5b00041
Inorg. Chem. XXXX, XXX, XXX–XXX

the best of our knowledge, this compound is the first radical-doped polyoxometalate-based host−guest multifunctional crystalline material with photochromism, photocontrolled tunable luminescence, and photocatalytic activity.

EXPERIMENTAL SECTION

Synthesis of *N*,*N*′-di(4-pyridyl)-1,4,5,8-naphthalenediimide (DPNDI) tectons. The mixture of 1,4,5,8-naphthalene-tetracarboxylic dianhydride (3 mmol) and 4-aminopyridine (6 mmol) in dimethylformamide (DMF, 20 mL) was heated under reflux for 8 h. When the reaction mixture reached room temperature, a crystalline solid precipitated and was then collected by filtration. The crude product was purified by recrystallization from DMF to obtain DPNDI as off-white crystalline solids.[8]

Synthesis of compound **1**. A solution (1 mL) of *N*-methyl-2-pyrrolidone (NMP)/MeCN (1:1, v/v) was carefully layered over an NMP (2 mL) solution of DPNDI tectons (0.03 mmol, 0.0126 g), and then the solution of $ZnSiF_6$ (0.057 mmol, 0.0127g) and $H_3PW_{12}O_{40}$ (0.017 mmol, 0.05g) in MeCN/MeOH (2:1, v/v, 3 mL) mixture was carefully added as a second layer. Yellow crystals that appeared after several days were collected and washed with MeCN in ca. 65% yield (based on Zn). Crystal data and the structure refinements are summarized in Table 1S (see the Supporting Information). Elemental analyses of C, H, and N were performed with a Vario EL III elemental analyzer. Anal. Calcd for $C_{88}H_{100}F_4W_{24}N_{16}O_{96}P_2Zn_3$: C 13.78, H 1.32, N 2.92%. Found: C 14.95, H 1.26, N 3.64%. The difference was probably because of the volatile solvent molecules in the frameworks. Combined with molecular weight calculator, the result we calculated is that there are approximately five MeCN molecules. Calcd: C 14.96, H 1.47, N 3.74%. Elemental analyses of Zn and W were performed with Ultima2 inductively coupled plasma OES spectrometer. Anal. Calcd for $C_{88}H_{100}F_4W_{24}N_{16}O_{96}P_2Zn_3$: Zn 2.49, W 56.07% (including five MeCN molecules). Found: Zn 2.53, W 55.98%. IR (cm^{-1}): 3438(m), 2931(w), 1639(s), 1510(w), 1346(m), 1244(m), 1063(m), 979(s), 822(s), 503(w).

RESULTS AND DISCUSSION

Structure of compound **1**. Single-crystal X-ray analysis reveals that compound **1** crystallized in the *P*4/*nnc* space group. The center Zn(II) ion is octahedrally coordinated by two bridging fluorine atoms (Figure 1a) and four nitrogen atoms from four functionalized π-electron-deficient DPNDI tectons. The other nitrogen atoms from the bridging DPNDI tectons coordinated with neighboring zinc ions to generate a two-dimensional (2D) grid structure. Additional two Zn(II) ions, which are perpendicular to the 2D grid network, are linked by the two bridging fluorine atoms (Figure 1a), respectively, then four solvent molecules (NMP) and one terminal fluorine atom occupy other coordination sites of Zn(II) to form a vertical bar, which looks like a railing. The Keggin polyanions ($[PW_{12}O_{40}]^{3-}$) not merely act as counterions but also serve as electron reservoirs; they typically reside directly over the electron-deficient naphthalenic ring centroid (centroid distance is ∼3 Å, Figure 1b; Figure S1 in the Supporting Information). The intermolecular weak C−H···anion interactions (hydrogen-bond geometry for **1** is available in the Supporting Information, Table S2) formed between pyridyl-H's of tectons (or hydrogen atoms of NMP molecules) and oxygen atoms from the POMs immobilize the functionalized POMs and enhance the stability of the structure. The POM anions along with several disordered solvent molecules filled in the gap of adjacent railings through obvious POM anion−π interactions.

The POM anion participates in anion−π interactions with two π-electron-deficient naphthalenic ring centroids (Figure S2 in the Supporting Information) of DPNDI tectons from

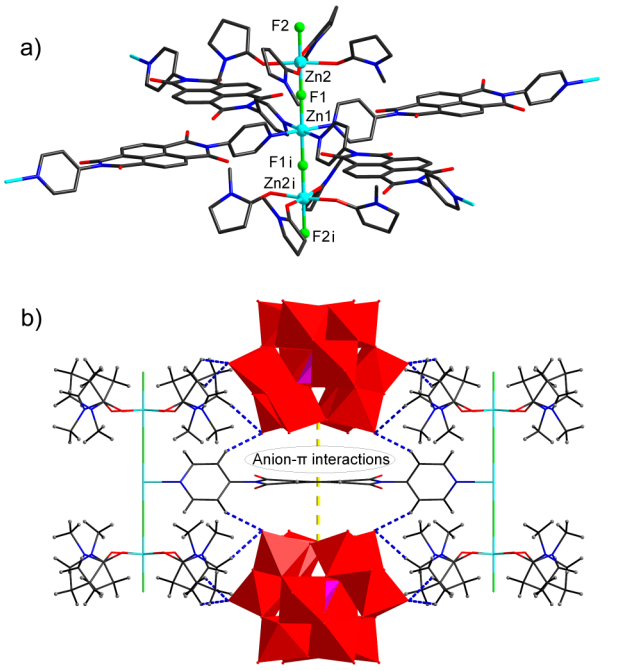

Figure 1. (a) Coordination environment of the Zn(II) ionic center in compound **1**. Symmetry codes: (i) *x*, 1.5 − *y*, 0.5 − *z*. (b) Anion−π (yellow dashed line) interactions between DPNDI and POMs, and C−H···anion (blue dashed line) interactions among components of **1**. Zn (turquoise), F (yellow-green), C (black), H (gray), O (red), N (blue), P (purple), W (teal), POMs (red and purple polyhedron).

contiguous network to generate a three-dimensional supermolecular structure (Figure S3 in the Supporting Information). In compound **1**, the POM anion is located on the line of the network (Figure S1 in the Supporting Information) rather than in the void of the two-dimensional (2D) network, which is much different than common POM-based host−guest 2D coordination polymer, that is, embedding POMs into the void of the coordination polymers, which is very sensitive to the pore size of the network.[9] On the other hand, each π-electron-deficient naphthalenic ring of DPNDI participates in anion−π interactions with two POM anions (Figure S2 in the Supporting Information) to construct a staggered POM-based host−guest structure, which is conducive to the formation of the novel railing-type host−guest coordination polymer so as to stabilize and disperse the trapped POM anions. Furthermore, these anion−π interactions will boost the electron transfer or exchange between NDI center and POM surface that helps to maintain POMs' efficient catalytic performance. The fraction of volumes accessible for the inclusion of guest solvent molecules is 29.3% (calculated by PLATON). Direct evidence for the inclusion of the guest solvent molecules was obtained by thermogravimetric analyses (TGA), which showed expected losses of mass in the range of 30−100 °C. The structure of **1** further demonstrated that electron reservoirs (POMs) can indeed be captured by π-electron-deficient naphthalenic ring of the DPNDI through obvious POM anion−π interactions. In a word, the railing of 2D quadrate network combined with the anion−π interactions between π-electron-deficient DPNDI tectons and the intermediate electron reservoirs (POMs) not only play crucial roles in stabilizing and directing formation of the novel POM-based host−guest coordination polymer but also increase the interactions between the components so as to accelerate the charge transfer and exchange to realize the fast-

DOI: 10.1021/acs.inorgchem.5b00041
Inorg. Chem. XXXX, XXX, XXX−XXX

responsive photochromism, photocontrolled luminescence, and photocatalytic activity.

Powder X-ray diffraction (PXRD) experiments on the bulk material of **1** show that all major peaks match well with simulated PXRD, indicating its crystalline phase purity (Figure S4 in the Supporting Information). TGA revealed that the weight loss of 2.73% from 30 to 100 °C is attributed to the desorption of five free MeCN molecules (calculated 2.61%). The weight loss of 10.2% from 200 °C to ∼400 °C may be attributed to the desorption of two end-coordinated fluorine ions and eight coordinated NMP molecules along the vertical railing (calculated 10.9%). Then the following weight loss from 400 °C corresponds to the collapse of coordination polymer (Figure S5 in the Supporting Information). Probably, the thermal stability of **1** is based on the following considerations: (i) there are some disordered solvent molecules (MeCN) in the coordination polymer; (ii) low noncovalent bond energy (the anion−π interactions between the POMs and rigid π-conjugated DPNDI tectons);[10] (iii) low bond energy between the Zn(II) ions and the coordinated solvent (NMP) molecules (or end-coordinated fluorine ions); (iv) the certain voids structure.

Photochromism. Interestingly, compound **1** (**1a**) is sensitive to sunlight and undergoes a photochromic transformation from yellowish to dark (**1b**) upon irradiation by ultraviolet visible light (Xenon Lamp, 300W, PLS-SXE 300/300UV, 320−780 nm) for a few seconds (Figure 2a). **1b** is stable in air and can return to yellow in a dark room for several minutes at ambient temperature. The analysis of electron spin resonance (ESR) spectra indicates that compound **1a** shows a weak peak radical signal with the g value of 2.0023 (Figure 2b). Compared with **1a**, **1b** exhibits a relatively strong sharp peak ESR signal of radicals, which suggests that there is a small amount of radicals in **1a** and that **1b** will rapidly generate amount of radicals after irradiated by ultraviolet visible light (**1b**, Figure 2b). In addition, the ESR spectra of compounds **1a** and **1b** both have a slightly wide weak peaks with the g value of 1.9278 (Figure 2b), which can be attributed to W(V) ions in the sample.[11] There was an obvious variation of the intensity of ESR signals of **1a** and **1b**. This variation most clearly illustrated that there are more radicals and W(V) ions after being irradiated by ultraviolet visible light. It is well-known that NDI derivatives are redox-active and can generate radicals upon light irradiation.[3g,12] It also has been known for a long time that POMs can act as electron reservoirs and be photochemically reduced to form colored mixed-valence species, and the process of formation of mixed-valence species is reversible.[4a] Thus, the photochromic process may mainly arise from photoinduced radical generation of organic tectons and the changes of valence state of metal ions of POMs. It must be pointed out that certain radicals and W(V) ions may occur in **1a** under the indoor natural light illumination; more specifically, the coordination polymer is a radical-doped material showing an obvious ESR signal, characteristic of imide radicals (g = 2.0032), which was present in the yellow crystalline solids without irradiation (Figure 2b). The Raman spectroscopy was employed to further probe changes in the vibrational frequencies accompanying redox state changes in the ligand cores. The Raman spectrum of **1a** exhibits one sharp peak at 1731 cm^{-1} (Figure S6 in the Supporting Information), which corresponds to the reported value (experiment value: 1726 cm^{-1} and calculated value: 1785 cm^{-1}) of the carbonyl stretching in partially reduced DPNDI (i.e., DPNDI radical anion).[12]

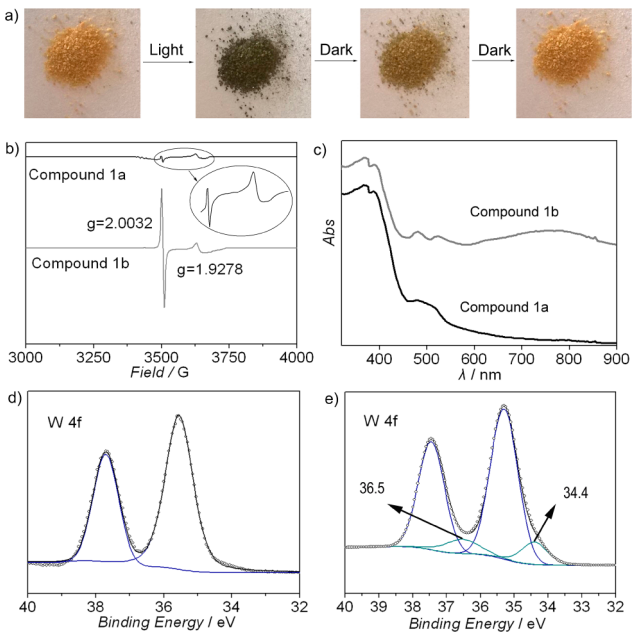

Figure 2. (a) The photochromic effect of the single crystal from photographic images. (b) ESR spectra for **1a** and **1b**. (inset) Enlarged ESR spectra of **1a**. (c) UV−vis spectra of **1a** and **1b**. (d) Resolved W 4f XPS core-level spectra of **1a**. (e) Resolved W 4f XPS core-level spectra of **1b**.

XPS analysis reveals that the tungstate experiences partial reduction under natural or ultraviolet visible light. In compound **1**, the main doublets of W 4f peak in **1a** (37.8 and 35.6 eV, Figure 2d) and **b** > **1b** (37.4 and 35.2 eV, Figure 2e) are located between the reported values of W(VI) ions and partial reduction of tungsten[13] that we have attributed to a partial reduction of tungsten under the natural light or ultraviolet visible light, which is consistent with the results of ESR of **1a** and **1b**. Compared with **1a**, the slight low-energy shifts of the XPS in **1b** relative to the reduction of tungsten are in accord with more W(V) ions in **1b** (Figure S7 in the Supporting Information). Note that, in **1b**, the W 4f peak displayed additional contributions at 36.5 and 34.4 eV (Figure 2e), which also can be contributed to more reduction of tungsten after ultraviolet light irradiation,[13] since the compound is sensitive to light; this is simply a matter of degree of reduction during light irradiation. Hence, it can be concluded that the photochromic process may also come from the changes of valence state of metal ions of POMs. There may be a charge transfer and exchange process among the components of this compound by the anion−π interactions and hydrogen bonds during irradiation.

UV−vis spectrum of **1a** and **1b** shows absorption bands at ∼380 nm, corresponding to the n−π* and π−π* transition of the aromatic organic tectons (Figure 2c). In addition, a weak shoulder around 500 nm can likewise be observed, which can be attributed to an intermolecular electron-transfer transition. The appearance of this band is consistent with the existence of the anion−π interactions and hydrogen bonds in the structure, which is considered to be a favorable condition for electron-transfer interactions. The UV−vis spectrum of **1b** displays a broad absorption band in the region of 600−850 nm, which may originate from a photoinduced electron-transfer transition.[3g] Therefore, besides the changes of valence state of

DOI: 10.1021/acs.inorgchem.5b00041
Inorg. Chem. XXXX, XXX, XXX−XXX

tungsten of POMs, the photochromic process may also arise from the photoinduced radical generation of organic ligands. That is to say, there are two reduction-active centers, which may accept electrons from the solvent molecules.

The cyclic voltammogram (CV) of compound **1a** exhibits one quasi-reversible processes in the cathodic region at $E_{1/2}$ = −0.874 V (Figure 3), which correspond to the reported

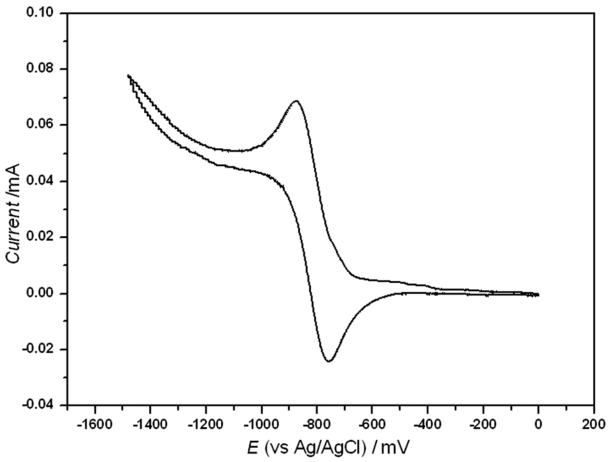

Figure 3. Solid-state CV of **1a** at 100 mV s^{-1} in a 0.1 M nBu$_4$NPF$_6$/MeCN electrolyte.

$[DPNDI]^{0/\bullet-}$ (−0.91 V) redox couples.[12] The reduction potential for $DPNDI^{\bullet-}$ formation in the coordination polymer is less negative than that of the DPNDI ligands. On the basis of Coulombic considerations, one would expect DPNDI reduction to be easier in MeCN than in the coordination polymer, because the charged anion radical should be stabilized in a polar solvent, in contrast to the hydrophobic environment of the stacked DPNDI molecules in the crystalline coordination polymer.[14] Since the opposite was observed, it can be supposed that DPNDI radical anions are stabilized in the crystalline solid material by delocalization of the unpaired electron over several molecules such as NMP molecules, POMs, and DPNDI molecules through anion−π interactions and hydrogen bonds, as proposed above for the radical-doped solids.

Luminescence. Considering the luminescence performance of DPNDI (Figure S8 in the Supporting Information), the d^{10} Zn(II) metal ion, and the photochromism of **1**, the photocontrolled luminescence of **1** was performed. As shown in Figure 4, compound **1** shows emission at 450 nm when excited at 350 nm. Interestingly, photocontrolled tunable luminescence was observed under the trigger of ultraviolet visible light. The strength of the emission of **1** was gradually reduced under ultraviolet visible light irradiation; as expected, the luminescence is almost quenching when the sample changes into dark after irradiating 15 s, but could be quickly recovered under dark for several minutes. This distinct behavior indicates that the photocontrolled tunable luminescence of **1** is reversible, which further demonstrates that there are electron-transfer interactions among the components of the compound during irradiation, thus resulting in weaker luminescence and even quenching.

Photocatalytic activity. The estimated band gap of compound **1** based on Kubelka−Munk Function is 2.83 eV (Figure 5a), which indicates that **1** can be bandgap photoexcited by simulated sunlight irradiation. As expected, a mild and green procedure for the photocatalytic oxidation of benzylic alcohols

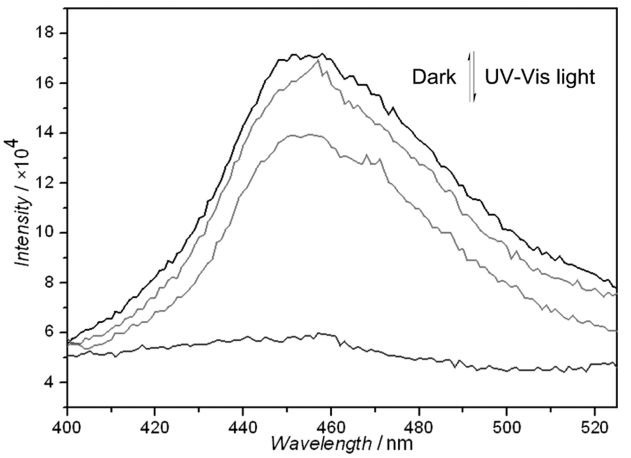

Figure 4. Photocontrolled tunable luminescence performance of **1** in the solid under UV−vis light (the spectrum was recorded of the samples under UV−vis light every 5 s or dark treatment).

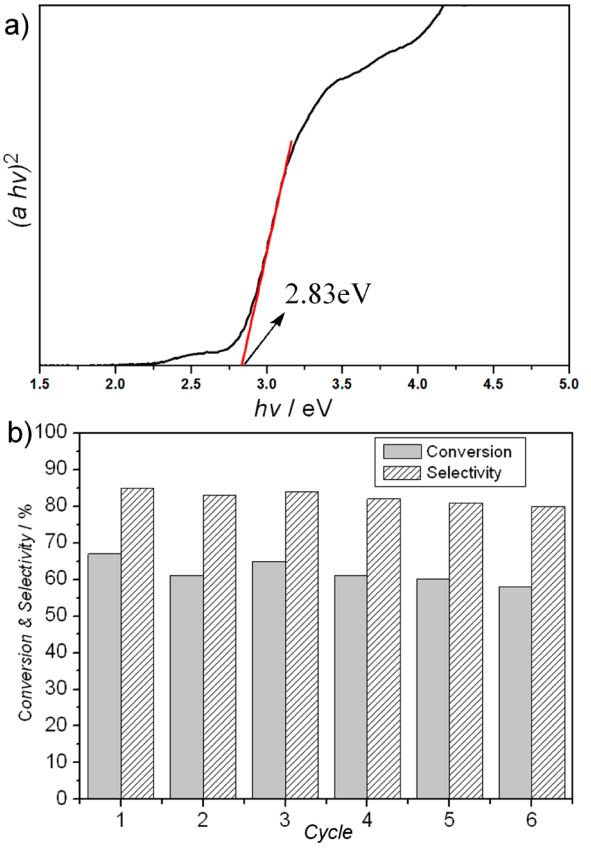

Figure 5. (a) The estimated energy band gap by the UV−vis diffuse reflectance spectroscopy based on the Kubelka−Munk Function. (b) Recycled photocatalytic oxidation of benzyl alcohol over compound **1**.

was achieved using this compound as a recyclable and eco-friendly heterogeneous photocatalyst in acetonitrile under air using ultraviolet visible light as the sole driving force (Scheme 1).

Experiments on photocatalytic selective oxidation of benzylic alcohols to corresponding aldehydes started with the reaction of benzyl alcohol. The time-online photocatalytic results for benzyl alcohol demonstrated that the high selectivity for benzaldehyde, ca. 85%, is obtained along with ca. 67% conversion under irradiating for 11 h (Figure S9 in the

DOI: 10.1021/acs.inorgchem.5b00041
Inorg. Chem. XXXX, XXX, XXX−XXX

Scheme 1. Selective Oxidation of Benzylic Alcohols

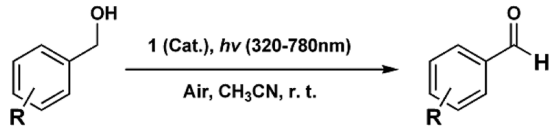

Supporting Information). The control experiments showed that no reaction occurred in the absence of compound **1** (Table 1, entry 2); therefore, the oxidation of benzyl alcohols is triggered by compound **1**, a photocatalyst. For comparison, a series of control photocatalysts were employed in the same photocatalytic experiments. The homogeneous catalyst $H_3PW_{12}O_{40}$ gave higher conversion (87%) under identical conditions; however, the selectivity to benzaldehyde was lower (69%) (Table 1, entry 3). Additionally, the recovery and recyclability of $H_3PW_{12}O_{40}$ was difficult. With $ZnSiF_6$–DPNDI, although comparable selectivity can be achieved, the conversion of benzyl alcohol was much lower than that with compound **1** (Table 1, entry 4). The recycling experiments suggested that compound **1** can be recovered easily by filtration. It can be reused in at least six runs without a significant decrease of conversion and selectivity (Figure 5b). The results suggest that compound **1** was more promising than its precursors as a photocatalyst. The combinations of the two major functional components not only improve the catalytic efficiency but also solve the problem of catalyst recycling. It is particularly worth mentioning that the selective photocatalytic oxidation of benzylic alcohols was performed at ambient condition using air as the sole catalyst reoxidant, which further suggests that compound **1** was an excellent heterogeneous photocatalyst.

Table 1. Photocatalytic Selective Oxidation of Various Benzylic Alcohols to the Corresponding Aldehydes with Compound 1 for 11 h

entry	R	catalyst	conversion (%)	selectivity[a] (%)
1	H	**1**	67	85
2	H		0	0
3	H	$H_3PW_{12}O_{40}$	87	69
4	H	$ZnSiF_6$-DPNDI	33	80
5	*p*-Me	**1**	53	>99
6	*p*-MeO	**1**	76	>99
7	*m*-Me	**1**	43	>99
8	*p*-F	**1**	50	83
9	*p*-Cl	**1**	63	>99
10	*p*-Br	**1**	56	>99
11	*p*-*i*Pr	**1**	45	>99
12	*p*-*t*Bu	**1**	40	>99

[a]Product identification was accomplished by Varian 4000 GC/MS or GC.

Selective oxidation of a variety of ring-substituted benzylic alcohols to corresponding aldehydes was also performed under similar reaction conditions; the results are listed in Table 1. Clearly, compound **1** is also active and highly selective for oxidation of ring-substituted benzylic alcohols. These results indicate that compound **1**, which combines multiple functional groups in a single structure, can be used as an excellent heterogeneous photocatalyst. This greatly improved photocatalytic activity may result from the unique structure features of the railing-type radical-doped host–guest material. The distinct POMs anion–π and C–H···anion interactions play an important role in incorporating functional components to construct multifunctional crystalline material as well as facilitating the charge transfer or exchange among internal components, which might be conducive to effectively improving the photocatalytic activity of POM-based host–guest materials in a mild and green experiment condition.

CONCLUSIONS

In conclusion, an extremely rare radical-doped POM-based host–guest crystalline material was reported for the first time, which has fast-responsive reversible photochromic properties varying from yellowish to dark and photocontrolled tunable luminescence. Moreover, an efficient procedure for the selective oxidation of benzylic alcohols or substituted benzylic alcohols has been developed using this POMs-based host–guest photochromic material as a green and recyclable photocatalyst under air as the sole catalyst reoxidant. Of particular importance is that the trapped POM anions connected with functional DPNDI tectons effectively via directional anion–π and C–H···anion interactions, which indicate POM anion–π interactions will not only be applicable to the stabilization and immobilization of the functional POM anions but also promote the charge transfer and exchange among components to lead to the reversible photochromism, photocontrolled tunable luminescence, and photocatalytic activity. All of these results indicate that it is a promising way to design and construct photochromic and photocatalytic crystalline materials based on multifunctional electron reservoirs (POMs) and π-electron-deficient NDIs dye derivatives by forming anion–π interactions.

ASSOCIATED CONTENT

Supporting Information

Experimental materials and physical measurements, crystallographic data, TGA, PXRD, solid-state Raman spectrum, XPS core-level spectra of **1**, additional figures, TEM images, and EDS of **1**, and hydrogen-bond geometry for compound **1**. This material is available free of charge via the Internet at http://pubs.acs.org.

AUTHOR INFORMATION

Corresponding Author

*E-mail: czlu@fjirsm.ac.cn. Fax: (+86)591-83714946. Phone: (+86)591-83705794.

Present Addresses

[§]Key Laboratory of Design and Assembly of Functional Nanostructures, Fujian Institute of Research on the Structure of Matter, Chinese Academy of Sciences, Fuzhou, Fujian 350002, P. R. China.

[⊥]Graduate University of Chinese Academy of Sciences, Beijing 100049, P. R. China.

Notes

The authors declare no competing financial interest.

ACKNOWLEDGMENTS

This work was supported by the 973 Key Program of the MOST (2012CB821705), the National Natural Science Foundation of China (21373221, 21221001, 91122027, 51172232, 21403236), the Chinese Academy of Sciences (KJCX2-YW-319 and KJCX2-EW-H01), and the Natural Science Foundation of Fujian Province (2012J06006 and 2006L2005).

DOI: 10.1021/acs.inorgchem.5b00041
Inorg. Chem. XXXX, XXX, XXX–XXX

REFERENCES

(1) (a) Pardo, R.; Zayat, M.; Levy, D. *Chem. Soc. Rev.* **2011**, *40*, 672−687. (b) Irie, M. *Chem. Rev.* **2000**, *100*, 5. (c) Wang, M. S.; Xu, G.; Zhang, Z. J.; Guo, G. C. *Chem. Commun.* **2010**, *46*, 361−376. (d) Zhang, H.; Chen, G.; Bahnemann, D. *J. Mater. Chem.* **2009**, *19*, 5089−5121. (e) Zhang, T.; Lin, W. *Chem. Soc. Rev.* **2014**, *43*, 5982−5993. (f) Wang, C. C.; Li, J. R.; Lv, X. L.; Zhang, Y. Q.; Guo, G. *Energy Envrion. Sci.* **2014**, *7*, 2831−2867.

(2) (a) Zou, C.; Zhang, Z. J.; Xu, X.; Gong, Q.; Li, J.; Wu, C. D. *J. Am. Chem. Soc.* **2012**, *134*, 87−90. (b) Férey, G.; Mellot-Draznieds, C.; Serre, C.; Millange, F. *Acc. Chem. Res.* **2005**, *38*, 217−225. (c) Rosseinsky, M. J. *Microporous Mesoporous Mater.* **2004**, *73*, 15−30. (d) Rowsell, J. L. C.; Yaghi, O. M. *Microporous Mesoporous Mater.* **2004**, *73*, 3−14. (e) Maspoch, D.; Ruiz-Molina, D.; Veciana, J. *Chem. Soc. Rev.* **2007**, *36*, 770−818. (f) Cheetham, A. K.; Rao, C. N. R.; Feller, R. K. *Chem. Commun.* **2006**, 4780−4795.

(3) (a) Dawson, R. E.; Henning, A.; Weimann, D. P.; Emery, D.; Ravikumar, V.; Montenegro, J.; Takeuchi, T.; Gabutti, S.; Mayor, M.; Mareda, J.; Schalley, C. A.; Matile, S. *Nat. Chem.* **2010**, *2*, 533−538. (b) Mareda, J.; Matile, S. *Chem.—Eur. J.* **2009**, *15*, 28−37. (c) Gorteau, V.; Bollot, G.; Mareda, J.; Perez-Velasco, A.; Matile, S. *J. Am. Chem. Soc.* **2006**, *128*, 14788−14789. (d) Guha, S.; Goodson, F. S.; Corson, L. J.; Saha, S. *J. Am. Chem. Soc.* **2012**, *134*, 13679−13691. (e) Guha, S.; Saha, S. *J. Am. Chem. Soc.* **2010**, *132*, 17674−17677. (f) Zhao, Y.; Domoto, Y.; Orentas, E.; Beuchat, C.; Emery, D.; Mareda, J.; Sakai, N.; Matile, S. *Angew. Chem., Int. Ed.* **2013**, *52*, 9940−9943. (g) Han, L.; Qin, L.; Xu, L.; Zhou, Y.; Sun, J.; Zou, X. *Chem. Commun.* **2013**, *49*, 406−408. (h) Nelson, A. P.; Farha, O. K.; Mulfort, K. L.; Hupp, J. T. *J. Am. Chem. Soc.* **2009**, *131*, 458−460. (i) Mulfort, K. L.; Hupp, J. T. *J. Am. Chem. Soc.* **2007**, *129*, 9604−9605. (j) Bhosale, S. V.; Jani, C. H.; Langford, S. J. *Chem. Soc. Rev.* **2008**, *37*, 331−342. (k) Katz, H. E.; Lovinger, A. J.; Johnson, J.; Kloc, C.; Siegrist, T.; Li, W.; Lin, Y. Y.; Dodahalapur, A. *Nature* **2000**, *404*, 478−481. (l) Wade, C. R.; Li, M.; Dincă, M. *Angew. Chem., Int. Ed.* **2013**, *52*, 13377−13381. (m) McCarthy, B. D.; Hontz, E. R.; Yost, S. R.; Voorhis, T. V.; Dincă, M. *J. Phys. Chem. Lett.* **2013**, *4*, 453−458.

(4) (a) Ymamse, T. *Chem. Rev.* **1998**, *98*, 307−326. (b) He, T.; Yao, J. *Prog. Mater. Sci.* **2006**, *51*, 810−879. (c) Dolbecq, A.; Dumas, E.; Mayer, C. R.; Mialane, P. *Chem. Rev.* **2010**, *110*, 6009−6048. (d) Liu, S.; Möhwald, H.; Volkmer, D.; Kurth, D. G. *Langmuir* **2006**, *22*, 1949−1951. (e) Walsh, J. J.; Mallon, C. T.; Bond, A. M.; Keyes, T. E.; Forster, R. J. *Chem. Commun.* **2012**, *48*, 3593−3595.

(5) (a) Miras, H. N.; Nadal, L. V.; Cronin, L. *Chem. Soc. Rev.* **2014**, *43*, 5679−5699. (b) Song, Y. F.; Tsunashima, R. *Chem. Soc. Rev.* **2012**, *41*, 7384−7402. (c) Zhou, Y.; Chen, G.; Long, Z.; Wang, J. *RSC Adv.* **2014**, *4*, 42092−42113. (d) Du, D. Y.; Qin, J. S.; Li, S. L.; Su, Z. M.; Lan, Y. Q. *Chem. Soc. Rev.* **2014**, *43*, 4615−4632. (e) Nisar, A.; Wang, X. *Dalton Trans.* **2012**, *41*, 9832−9845. (f) Lv, H.; Geletii, Y. V.; Zhao, C.; Vickers, J. W.; Zhu, G.; Luo, Z.; Song, J.; Lian, T.; Musaev, D. G.; Hill, C. L. *Chem. Soc. Rev.* **2012**, *41*, 7572−7589. (g) Kozhevnikov, I. V. *Chem. Rev.* **1998**, *98*, 171−198. (h) Long, D. L.; Tsunashima, R.; Cronin, L. *Angew. Chem., Int. Ed.* **2010**, *49*, 1736−1758. (i) Han, X. B.; Zhang, Z. M.; Zhang, T.; Li, Y. G.; Lin, W.; You, W. S.; Su, Z. M.; Wang, E. B. *J. Am. Chem. Soc.* **2014**, *136*, 5359−5366.

(6) (a) Sun, C. Y.; Liu, S. X.; Liang, D. D.; Shao, K. Z.; Ren, Y. H.; Su, Z. M. *J. Am. Chem. Soc.* **2009**, *131*, 1883−1888. (b) Ma, F. J.; Liu, S. X.; Sun, C. Y.; Liang, D. D.; Ren, G. J.; Wei, F.; Chen, Y. G.; Su, Z. M. *J. Am. Chem. Soc.* **2011**, *133*, 4178−4181. (c) Song, J.; Luo, Z.; Britt, D. K.; Furukawa, H.; Yaghi, O. M.; Hardcastle, K. I.; Hill, C. L. *J. Am. Chem. Soc.* **2011**, *133*, 16839−16846. (d) Han, Q.; He, C.; Zhao, M.; Qi, B.; Niu, J.; Duan, C. *J. Am. Chem. Soc.* **2013**, *135*, 10186−10189. (e) Liu, Y.; Liu, S.; Liu, S.; Liang, D.; Li, S.; Tang, Q.; Wang, X.; Miao, J.; Shi, Z.; Zheng, Z. *ChemCatChem* **2013**, *5*, 3086−3091.

(7) Lü, J.; Lin, J. X.; Zhao, X. L.; Cao, R. *Chem. Commun.* **2012**, *48*, 669−671.

(8) Liao, J. Z.; Dui, X. J.; Zhang, H. L.; Wu, X. Y.; Lu, C. Z. *CrystEngComm* **2014**, *16*, 10530−10533.

(9) Kong, X. J.; Ren, Y. P.; Zheng, P. Q.; Long, Y. X.; Long, L. S.; Huang, R. B.; Zheng, L. S. *Inorg. Chem.* **2006**, *45*, 10702−10711.

(10) (a) Chifotides, H.; Dunbar, K. R. *Acc. Chem. Res.* **2013**, *46*, 894−906. (b) Schottel, B. L.; Chifotides, H. T.; Dunbar, K. R. *Chem. Soc. Rev.* **2008**, *37*, 68−83. (c) Jentzsch, A. V.; Henning, A.; Mareda, J.; Matile, S. *Acc. Chem. Res.* **2013**, *46*, 2791−2800. (d) Quiñonero, D.; Garau, C.; Rotger, C.; Frontera, A.; Ballester, P.; Costa, A.; Deyà, P. M. *Angew. Chem., Int. Ed.* **2002**, *41*, 3389−3392. (e) Alkorta, I.; Rozas, I.; Elguero, J. *J. Am. Chem. Soc.* **2002**, *124*, 8593−8598.

(11) (a) Prados, R.; Pope, M. T. *Inorg. Chem.* **1976**, *15*, 2547−2553. (b) Varga, G. M., JR.; Papaconstantinou, E.; Pope, M. T. *Inorg. Chem.* **1970**, *9*, 662−667.

(12) Leong, C. F.; Chan, B.; Faust, T. B.; D'Alessandro, D. M. *Chem. Sci.* **2014**, *5*, 4724−4728.

(13) (a) Mercier, D.; Boujday, S.; Annabi, C.; Villanneau, R.; Pradier, C. M.; Proust, A. *J. Phys. Chem. C* **2012**, *116*, 13217−13224. (b) Legagneux, N.; Basset, J. M.; Thomas, A.; Lefebvre, F.; Goguet, A.; Sá, J.; Hardacre, C. *Dalton Trans.* **2009**, 2235−2240. (c) Wagner, C. D.; Riggs, W. M.; Davis, L. E.; Moulder, J. F.; Muilenberg, G. E. *Handbook of X-ray Photoelectron Spectroscopy;* Perkin-Elmer Corporation, Physical Electronics Division: Waltham, MA, 1979. (d) Nagaoka, Y.; Shiratori, S.; Einaga, Y. *Chem. Mater.* **2008**, *20*, 4004−4010.

(14) (a) Brochsztain, S.; Rodrigues, M. A.; Demets, G. J. F.; Politi, M. J. *J. Mater. Chem.* **2002**, *12*, 1250−1255. (b) Thalacker, C.; Röger, C.; Würthner, F. *J. Org. Chem.* **2006**, *71*, 8098−8105.

DOI: 10.1021/acs.inorgchem.5b00041
Inorg. Chem. XXXX, XXX, XXX−XXX